

MASTER

FERMI SURFACE MEASUREMENTS IN ACTINIDE METALS AND COMPOUNDS

by

A. J. Arko and J. E. Schirber

NOTICE
This report was prepared as an account of work
sponsored by the United States Government. Neither the
United States nor the United States Department of
Energy, nor any of its employees, nor any of their
contractors, subcontractors, or their employees, makes
any warranty, express or implied, or assumes any legal
liability or responsibility for the accuracy or completeness
of any information, apparatus, product, or process
disclosed, or represents that its use would not
infringe privately owned rights.

Prepared for

3rd International Conference on
the Electronic Structure of the Actinides
Grenoble, France
August 30 to September 1, 1978



ARGONNE NATIONAL LABORATORY, ARGONNE, ILLINOIS

Operated under Contract W-31-109-Eng-38 for the
U. S. DEPARTMENT OF ENERGY

FERMI SURFACE MEASUREMENTS IN ACTINIDE METALS AND COMPOUNDS*

A. J. Arko

Argonne National Laboratory, Argonne, IL 60439

and

J. E. Schirber

Sandia Laboratories, Albuquerque, N.M. 87110

ABSTRACT

The various techniques of measuring Fermi Surface parameters are briefly discussed in terms of application to actinide systems. Particular emphasis is given the dHvA effect. Some general results found in the dHvA studies of actinide compounds are given. The dHvA effect has been measured in α -U and is presented in detail. None of the observed frequencies corresponds to closed surfaces. Results are compared to the calculations of Freeman, Koelling and Watson-Yang where qualitative agreement is observed.

Les diverses techniques de mesure des paramètres de surface de Fermi sont ici discutées du point de vue de l'application aux systèmes actinides. L'effet dHvA a été plus particulièrement étudié. Quelques résultats d'ordre général issus de l'étude dHvA des composés actinides sont exposés. L'effet dHvA a été mesuré dans l'U- α . Il est ici présenté en détail. Aucune des fréquences observées ne correspond à celles des surfaces fermées. Les résultats s'accordent qualitativement avec les calculs de Freeman, Koelling et Watson-Yang.

I. Introduction

Measurements of the Fermi surface of metals have proven extremely successful in understanding the electronic properties of simple and transition metals.⁽¹⁾ The de Haas-van Alphen (dHvA) effect, in particular continues to be the most precise measurement of the Fermi surface

parameters and a check on band structure calculations. However, the techniques which worked so well for the simpler metals are not always as effective when applied to the very complex actinide systems. For example, the necessity of dealing relativistically with upwards of 20 conduction electrons per unit cell almost precludes a self-consistent band calculation. Thus even in those infrequent cases where sufficiently pure samples are available to yield dHvA data, one is hard-pressed to obtain as much information as is obtainable in simpler systems.

Nevertheless considerable progress has been made in actinides. The dHvA effect has been observed in the compounds URh_3 ,⁽²⁾ UIr_3 ,⁽³⁾ UGe_3 ,⁽⁴⁾ UAl_2 , and U_3As_4 , and in the metals Th ⁽⁵⁾ and $\alpha-U$.⁽⁶⁾ New results on $\alpha-U$ will be discussed in detail in this paper.

It is the purpose of this paper to review the progress of the work to date with particular emphasis on the $\alpha-U$ research and to indicate the prospects of "Fermiology" and band structure studies in future actinide research. The discussion of compounds will be very brief.

In Section II we give a brief overview of the Fermi surface program and the applicability of each type of measurement to actinides with the dHvA effect considered in some detail. We will not be concerned in this paper with the fine points of the motion of electrons in a strong magnetic field. We will look at the dHvA effect merely as a tool in the investigation of materials. In Sec. III we consider the results obtained in actinide compounds via the dHvA effect, while the special case of $\alpha-U$ is given considerable attention in Sec. IV.

II. Available Measuring Techniques

A large arsenal of tools is available to the Fermiologist to obtain various types of information about the Fermi surface. Because of space requirements it will not be possible to discuss each type in de-

tail except to mention the parameters measured. Volumes of articles are written on the subject with one of the best being the Simon Fraser Lecture Series.⁽¹⁾

The various measurements may be broadly separated into two groups including: (1) Traditional tools, requiring use of magnetic fields, high purity single crystals, and essentially depending on the quantization of orbits in the plane normal to H at low temperatures, and (2) alternate approaches utilizing positrons, photons or neutrons as momentum probes, generally at room temperature. The latter group lacks the precision obtainable in the former, but it has the distinct advantage of far less stringent sample requirements. In the case of actinide materials this may yet prove to be the overriding factor since some information is better than none.

Let us discuss each group in somewhat more detail.

A. Traditional Measurements

We name here only the most frequently used measurements. These include magnetoresistance,⁽⁷⁾ cyclotron resonance,⁽⁸⁾ various dc size effects,⁽⁹⁾ rf size effect,⁽¹⁰⁾ magneto-acoustic effect,⁽¹¹⁾ magnetostriction,⁽¹²⁾ magnetocaloric effect,⁽¹³⁾ and the dHvA effect. The first five are somewhat specialized, yielding information respectively (in the plane normal to H) on the topology of the Fermi Surface, effective mass (m^*) of electrons, Fermi surface curvature, and the caliper diameter of the Fermi surface.^(5,6) The quantized nature of electron orbits in a magnetic field can be utilized to produce any number of resonances under specialized conditions. While these are interesting from a phenomenological point of view, most of them are impractical in the study of compounds where $\omega_c \tau$ (ω_c is the cyclotron frequency = eH/m^* and τ is the relaxation time) is not much larger than ~ 1 .

The resonance phenomena depend on power absorption at a frequency $\omega = \omega_c$ by a periodic sampling by the electrons of the specimen surface (the skin depth region). If τ is small only one such sampling will occur before scattering. Except for magnetoresistance, where information can be obtained once one satisfies the conditions $\omega_c \tau \gtrsim 1$, the sample purity requirements are in general beyond those obtainable in even simple metal compounds, much less so in actinide compounds, and are thus of little practical value for our purposes. The remaining three types of measurements are in principle closely related to each other. Although, because of the simplicity of the dHvA effect relative to the others, it has been and will continue to be the most useful.

Of these traditional tools, only magnetoresistance⁽¹⁴⁾ and the dHvA effect^(2,3,4,6) have been successfully applied in the study of actinide materials. Since magnetoresistance (or more generally, galvanomagnetic effects) can only consider a few specific points (namely, the topology of the Fermi surface and the relative number of holes vs electrons) it becomes useful only as a first step in the Fermi Surface determination, or to resolve topological questions as in the case of UGe_3 .⁽¹⁴⁾

It is obvious that of the measurements relying on the quantization of orbits, the dHvA effect is most practical. Results can be obtained whenever $\omega_c \tau \gtrsim 1$. It yields most of the information obtainable with other techniques either directly or indirectly. Its accuracy is far greater than needed to gauge the present band-structure calculations. Much has been written about the dHvA effect and the reader is referred to excellent review articles in the Simon Fraser Lecture Series.⁽¹⁾

B. Experiments Utilizing Momentum Probes

This is an enormous topic, the detailed descriptions being well beyond the scope of this paper. We will only mention the more popular experiments and the type of information obtained. The usual momentum probes are in the form of neutrons, positrons, electrons, photons and even ions.

Measurements of the pseudopotential form factor $V(\vec{q})$ have been successfully done with neutrons,⁽¹⁵⁾ but aside from that, little Fermi surface data are obtained utilizing neutrons. Ion neutralization spectroscopy⁽¹⁶⁾ likewise is little utilized.

The most promising techniques, particularly for actinides where pure crystals are difficult to obtain, are position annihilation⁽¹⁷⁾ and angular resolved photoemission spectroscopy.⁽¹⁸⁾ With great improvement in counting techniques, and hence statistics, positron annihilation has the potential of supplanting dHvA as the premiere Fermiology tool. It is still far from that at this time, however.

Angular resolved photoemission spectroscopy has demonstrated the capability of actually mapping out the energy bands near the Fermi level with some precision. This technique, together with the dHvA effect and possibly positron annihilation is likely to provide great new strides in the field of Fermiology.

In the remaining portions of this paper we will be concerned with particular applications of the dHvA effect.

III. Actinide Compounds

Before we consider the case of α -U, let us briefly review some of the work on compounds, present some general findings for the class of Ll_2 materials, and discuss some prospects for the future.

Complete dHvA data have been obtained for $URh_3^{(2)}$, $UIr_3^{(3)}$ and $UGe_3^{(4)}$. In the first two cases, the agreement between theory and experiment is qualitative, while in the case of UGe_3 it is excellent. Indeed, in UGe_3 the complex Fermi surface could only be determined with the aid of the band structure predictions. From these studies the following conclusions were drawn: 1) f-bands in these systems are broadened via hybridization with d- or p- electrons, forming σ bonds in the former, and π bonds in the latter. This quenches the magnetism one would expect to find on the basis of actinide-actinide separation; 2) The Fermi level in UGe_3 lies at a sharp peak in the density of states and is responsible for the spin fluctuation phenomena.⁽¹⁹⁾ This contrasts with the broad peak at E_F in URh_3 and UIr_3 . 3) In the UGe_3 compound the U-atom gives up 3 electrons to the 3 Ge atoms and is in the configuration $U^{3+}(f^2d^1)$. Similar charge transfer has also been invoked to explain neutron diffraction results⁽²⁷⁾ in URh_3 . In general all bulk property data can be understood on the basis of the band structures found in these systems.

dHvA measurements become more difficult as one proceeds to materials with more complex structures and large specific heat γ -values. Limited dHvA data have been obtained in U_3As_4 and in UAl_2 , the latter done in a pulsed field to 400 kOe. (A field sweep of the UAl_2 data is shown in Fig. 1.) It is becoming apparent that in future research on these systems it may be necessary to utilize momentum probes or very large magnetic fields since very large effective masses seem to be the rule rather than the exception. In U_3As_4 , for example, an orbit with

only a 1×10^7 Gauss frequency (nearly isotropic and the only one observed) had $m^* \approx 5 m_0$. The large masses, coupled with the chemical reactivity of the actinides, which causes an obvious purification problem, will probably necessitate that most future dHvA work will have to be done at fields in excess of 200 kOe. As Fig. 1 shows, such data are feasible. The curve of Fig. 1 is all the more remarkable since the specimen⁽²¹⁾ has $\gamma = 100 \text{ m J/mole K}^2$ and a residual resistance ratio (RRR) of only 18 at 4.2°K. This clearly represents rather extreme conditions. The observed frequency was small (5×10^6 Gauss) and no mass measurements were made, but it nevertheless shows that the band structure of high - γ actinide compounds can be studied in this manner.

In the dHvA study of these complex materials one wished to examine those systems for which band structure calculations are feasible and good crystals can be prepared. There are a surprisingly small number of such compounds of uranium. There are, however, a number of congruent-melting Pu compounds with low γ -values and cubic symmetry which offer hope for future research. Also a number of compounds having the NaCl structure exist but crystals have not yet been prepared of sufficient purity. Once the sample problem is solved additional dHvA work can be carried out.

IV α - URANIUM

Attempts to observe dHvA oscillations in α -U in the past were thwarted by several phase transitions which occur at 43 K (second order), 37 and 23 K (first order).⁽²²⁾ Resistivity measurements indicated⁽²³⁾ that defects and dislocations introduced by incomplete phase transitions were present even when the sample was cooled slowly through these transitions. Since the dHvA effect is particularly sensitive to defects and other small-angle scattering events not

seriously affecting resistivity, it is not surprising that a total suppression of the dHvA amplitudes occurs, particularly since effective masses are large.

From the pressure studies of Fisher and Dever⁽²⁴⁾ it was determined by a straight line extrapolation that the 43 K transition can be totally suppressed at 10-12 kbar. This encouraged us to attempt to quench the phase transitions with hydrostatic pressure (imperative, since α -U crystallizes in an orthorhombic lattice with highly anisotropic compressibilities and thermal expansivities) using the solid He pressure technique.⁽²⁷⁾

dHvA oscillations are observed just above 8.3 kbar making it tempting to infer that the second-order phase transition is suppressed at that point. A T_c vs pressure curve (Fig. 2) was obtained to determine the pressure phase diagram using the dHvA samples themselves. (The data of Smith and Fisher⁽²⁶⁾ and Palmy and Fisher⁽²⁷⁾ are superimposed in Fig. 2 for comparison.) Clear transitions were seen at 6.3 kbar and 7.1 kbar. However, the lack of a slope change at 8.3 kbar allows some ambiguity that the onset of the dHvA oscillations at 8.3 kbar is due to a total suppression of all phase transformations. We nevertheless believe that this is indeed the case, and that our dHvA data are obtained in the uranium α -phase.

Initial observation of the dHvA effect occurred already⁽⁶⁾ in 1974. However, our fixed geometry did not allow angular variation. In the present experimental arrangement a split coil superconducting magnet (100 kOe) which can be rotated in the horizontal plane was used to obtain angular data. The samples were placed in a transverse pickup coil having dimensions of 0.75 mm I.D. x 2.5 mm O.D. x 2.0 mm long, with both sample and pickup coil contained inside a 3 mm dia. pressure bomb.

Data were taken at $\approx 1^\circ\text{K}$ using the usual field modulation technique. Because of the orthorhombic symmetry it was necessary to take data in all three orthogonal planes for the full 90° range.

Results are shown in Fig. 3. Five frequency branches were observed with the data obtained from rotation diagrams, direct frequency analysis, beat analysis, and Fourier analysis. From the figure one can see close agreement from all modes of measurement.

None of the observed frequencies are due to closed pieces of Fermi surface. In fact, α , β , and δ are very reminiscent of neck-like structures or tubes. Frequency α varies almost precisely as a cylindrical piece of Fermi surface, i.e., one whose cross-sectional area does not change along the field axis. Frequency β varies much slower than a cylinder which would indicate that the cylinder has some undulations and that for $H \parallel [100]$ the observed extremal orbit passes around the thick part of the undulation. Frequency δ varies much faster than a cylinder which leads to a similar interpretation except that for $H \parallel [001]$ the extremal orbit goes around a waist of an undulating cylinder.

Frequencies γ and ϵ are both very weak with γ observable only as a beat on top of the much stronger α -frequency (all signals in fact are extremely weak except for α at $[010]$ and β at $[100]$). It is not clear whether frequency branch ϵ is an independent branch or whether it is part of branches γ or α . Both of these latter branches can be extrapolated through the gaps in the data to ϵ , and indeed all three may be related. Occurrence of gaps in the frequency spectrum is not unusual (see for example, data in Ref. 2) and is usually due to some protrusions or extensions on the Fermi surface.

Effective masses for α -U are shown in Table I for orientations where measurements were possible. It will be seen that in general the masses are large, the smallest being $0.9 m_0$ for frequency branch β at $\{100\}$. From this one would anticipate that perhaps there are still higher masses on several as yet unobserved orbits. But considering the small size of the Brillouin zone and using the model of the Fermi surface of Freeman et al.⁽²⁸⁾ (reported elsewhere at this conference) as a guide, it will be seen below that perhaps we have observed a sizable fraction of the extremal orbits in α -U.

Freeman, Koelling and Watson-Yang⁽²⁸⁾ have performed a band structure calculation for orthorhombic α -U using the relativistic linearized augmented plane wave method. While no attempt at self-consistency was made, (they assumed an $f^3 d^2 s^1$ configuration) the results are nevertheless a good starting point in interpreting the dHvA data. As we will see, qualitative agreement does seem to exist.

Figs. 4 and 5 are cross sections through the Brillouin Zone of orthorhombic α -U showing the theoretically predicted Fermi surfaces. Band 6 in Fig. 4 nearly fills the zone resulting in a hole surface which is open in the c-direction. Two cross-sections are shown: (a) at the center of the zone ($z = 0$) and (b) at the top of the zone ($z = 1$). Clearly this is an undulating tube with a waist at the $z = 1$ point. Closed electron trajectories are possible for $H \parallel [001]$ both at $z = 0$ and $z = 1$. Figs. 5a and 5b show an electron surface coming from band 7, again at $z = 0$ and $z = 1$. Fig. 5c shows a view along the b axis for $y = 0$. One can see that this is again an open surface in the c-direction, but this time closed electron trajectories are possible for

H both along the a- and b- axes as well as the c-axis (see Fig 5c). In particular, a hole orbit (ζ) is possible for H near b and at least one electron orbit (dotted curve labeled η in Fig. 5c) around the central section of the Fermi Surface for H near a (if the small pocket in the center of the zone is ignored). The very large central orbit in band 7 for H||c would probably have too large a mass to be observed. Its cross-sectional area would be two to three times larger than all observed frequencies.

Let us now consider the correspondence between the predicted and experimentally observed results and confine ourselves to qualitative rather than quantitative comparisons. The first thing to note is that there are no closed surfaces predicted nor observed. The cross-sectional areas are approximately in agreement with observation (see Fig. 5d for size of cross-sectional area corresponding to a 2.12×10^7 Gauss frequency) if we ignore the very small pockets and the very large orbits, the latter being difficult to observe. The waist extremal orbit on the band six hole surface at $z = 1$ (Fig. 4b) could very well correspond to the observed δ frequency (frequency increases much faster than for a cylinder). The lack of observation of the larger extremal belly orbit at $z = 0$ is not a serious drawback since one can argue that one has large effective masses. The waist orbit was already just at the edge of observability so that the amplitude of any larger orbit would probably be too small for our experimental apparatus.

Along the b-axis two frequencies are observed. The nearly cyclindrical variation of frequency α would imply that the surface has very flat sides. This is more or less the case for the hole orbit ζ in Fig. 5c. One might then associate frequency branch α with the hole orbit ζ .

There is at present no explanation ⁽²⁸⁾ for frequency branch γ . Due to the gap in the data it is not even certain if it extends into the b-axis. It might be pointed out, however, that bands 6 and 7 approach each other very closely at the point H in the zone, particularly somewhat below the $z = 1$ point. This could allow for magnetic breakdown between the two sheets for H near the b-axis and explain the very weak amplitudes of γ .

Frequency branch β could correspond to the orbit η (dashed line in Fig. 5c) if the small central pocket at Γ is ignored. The area of this orbit would increase slower than for a cylinder. Only a small change in the band structure is needed to eliminate the Γ pocket, well within the error of the calculation. Since small pockets should be relatively easy to observe, lack of observation can be taken to mean lack of existence.

A very bothersome point is the failure to observe a frequency corresponding to an orbit around the arm of the band 7 surface for $H \parallel [101]$. We must resort to our oft-repeated statement that the effective mass must be large for this orbit although for this case the statement is not very satisfactory. A calculation of the masses for the orbits discussed above could be useful in obtaining further correspondence between theory and experiment in the future.

In summary then, it is seen from the α -U results that dHvA data serve as a powerful tool in determining band structure. Since the calculations of Freeman et al. show the qualitative features of the observed data, they can serve as a guide in interpreting other data. Further calculational refinements are likely to be minor, such as elimination of the pockets at Γ .

We wish to thank Drs. A. J. Freeman, D. D. Koelling and
T. J. Watson-Yang for use of their calculations prior to publi-
cation and for numerous helpful discussions.

Figure Captions

Fig. 1 Dual recorder tracing of a magnetic field pulse to 400kOe showing the field strength (upper trace) and pickup-coil output (lower trace). Note dHvA oscillations from UAl_2 in the lower trace.

Fig. 2 Pressure vs. superconducting critical temperature (T_c) in α -U using dHvA samples themselves. Previous data⁽²⁶⁾⁽²⁷⁾ are also shown.

Fig. 3 dHvA frequency spectrum for α -U in the three orthogonal planes.

Fig. 4 α -U band 6 hole surface and Brillouin zone cross-section in the (001) plane (after Freeman et al.): a) at $z = 0.0\pi/c$ and b) at $x = 1.0\pi/c$.

Fig. 5 α -U electron surface and Brillouin zone cross sections (After Freeman et al.): a) (001) plane at $z = 0.0\pi/c$; b) (001) plane at $z = 1.0\pi/c$; c) (010) plane at $y = 0.0\pi/b$; d) Cross-sectional area corresponding to a frequency of 21.2×10^6 Gauss, using same scale as Figs. a, b and c.

REFERENCES

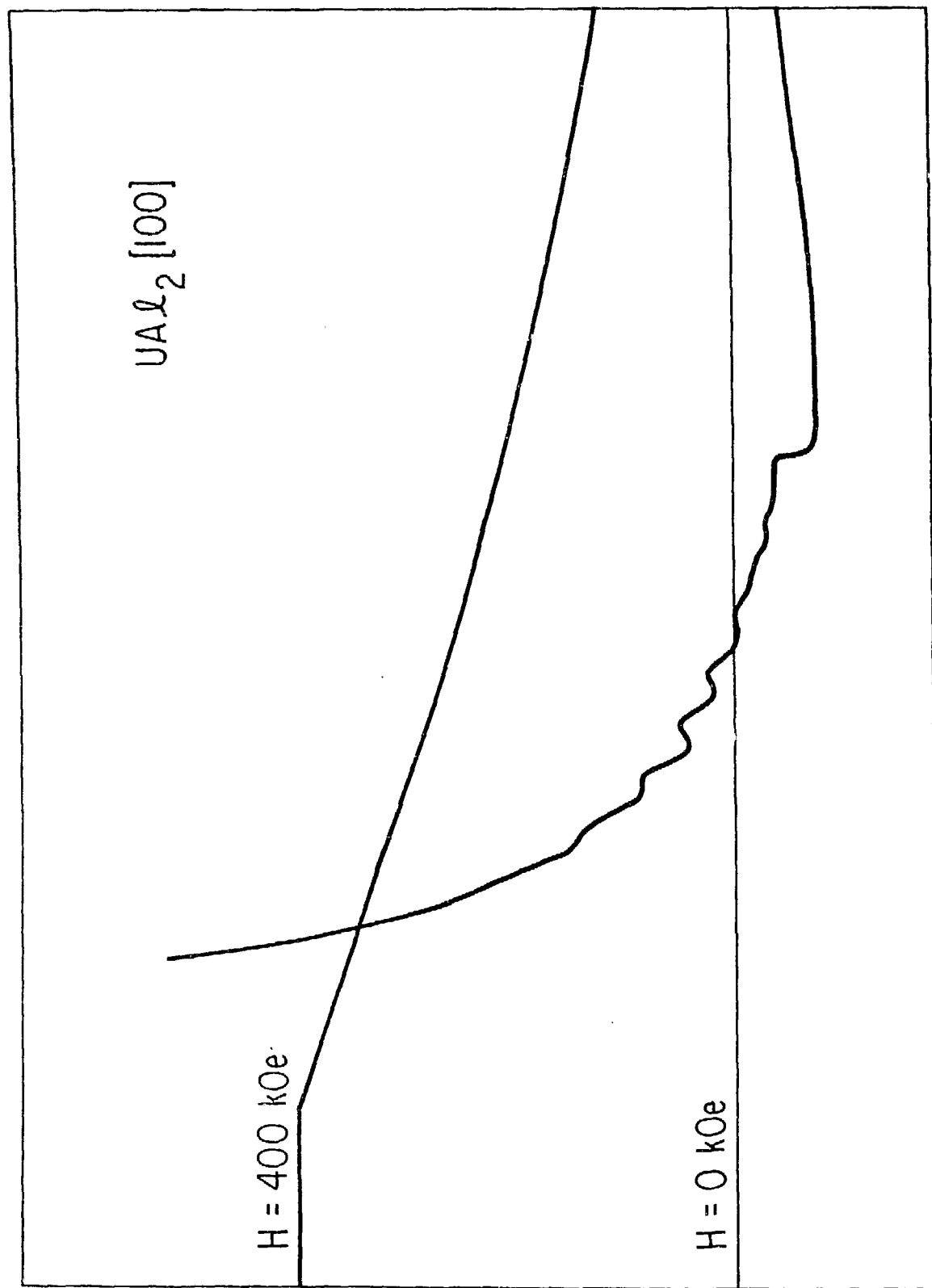
- * Work supported by the U.S. Department of Energy.
1. See for example Solid State Physics - The Simon Fraser University Lectures, Vol. 1, Cochran, J. F., and Haering, R. R. eds., Gordon and Breach (New York, 1968), and references therein.
 2. Arko, A. J., Brodsky, M. B., Crabtree, G. W., Karim, D., Koelling, D. D., and Windmiller, L. R., Phys. Rev. B 12 (1975) 4102.
 3. Arko, A. J., Brodsky, M. B., Crabtree, G. W., Karim, D., Windmiller, L. R., and Ketterson, J. B., Plutonium 1975 and Other Actinides, edited by H. Blank (North Holland, Amsterdam, 1976) 325.
 4. Arko, A. J. and Koelling, D. D., Phys. Rev. B 17 (1978) 3104.
 5. Schirber, J. E., Schmidt, F. A. and Koelling, D. D., Phys. Rev. B 16 (1977) 9235.
 6. Schirber, J. E., Arko, A. J. and Fisner, E. S., Solid State Comm. 17 (1975) 553.
 7. Fawcett, E., Advan. Phys. 13 (1964) 139.
 8. Walsh, W. M., Ref. 1, Ch. 3.
 9. Gurevich, V. L., Soviet Phys. JETP 8 (1959) 464.
 10. Gantmakher, V. F., Progress in Low. Temp. Phys., edited by Gorter, C. J. (North Holland, Amsterdam, 1967) Vol. V. 181.
 11. Ketterson, J. B. and Stark, R. W., Phys. Rev. 156 (1967) 748.
 12. Chandrasekhar, B. S., Phys. Letters 6 (1963) 27.
 13. Kunzler, J. E., Hsu, F. S. L. and Boyle, W. S., Phys. Rev., 128 (1962) 1084.
 14. Gerber, J. A., Sellmeyer, D. J. and Arko, A. J., J. Low Temp. Phys. 29 (1977) 345.
 15. Chambers, R. G., Ref. 1, Ch. 5, and references therein.

REFERENCES - Page 2

16. Hagstrum, H. D., Phys. Rev. 150 (1966) 495.
17. Stewart, A. T., Positron Annihilation, edited by Stewart, A. T. and Roelling. L. O. (Academic, New York, 1967).
18. See for example Williams, P. M., Butcher, P. and Wood, J., Phys. Rev. B 14 (1976) 3215.
19. Buschow, K. H. J. and van Daal, H. J., AIP Conf. Proc. 5 (1971) 1464.
20. Delapalme, A., Lander, G. H. and Brown, P. J., J. Phys. C 11 (1978) 1441.
21. Trainor, R. J., Brodsky, M. B. and Culbert, H. V., Phys. Rev. Lett. 34 (1975) 1019.
22. Steinitz, M. O., Burleson, C. E. and Marcus, J. A., J. Appl. Phys. 41 (1970) 5057.
23. Jousset, J. C. and Quere, Y., Phys. Lett. 5 (1963) 238.
24. Fisher, E. S., and Dever, D., Phys. Rev. 170 (1968) 607.
25. Schirber, J. E., Cryogenics 10 (1970) 418.
26. Smith, T. F. and Fisher, E. S., J. Low Temp. Phys. 12 (1973) 631.
27. Palmy, C. and Fisher, E. S., Solid State Com. 8 (1970) 655.
28. Freeman, A. J., Koelling, D. D. and Watson-Yang, T. J., This conference.

Table I Effective mass ratios of various sheets of the Fermi surface of U for minimum area field directions. Data were taken near 9.0 kbar.

Fermi surface sheet	Field direction	Frequency in 10^6 G	Effective mass ratio
α	[010]	12.96	0.91
β	[100]	13.9	0.9
γ	70 deg from [001] in (100)	19.2	1.8
δ	[001]	21.2	1.8



TIME

